Electronic Supplementary Material (ESI) for Physical Chemistry Chemical Physics.

Electronic Supplementary Information for Understanding the Luminescence Properties of Cu(I) Complexes: A Quantum Chemical Perusal

Nora Lüdtke, Jelena Föller, and Christel M. Marian*

Institut für Theoretische Chemie und Computerchemie, Heinrich-Heine-Universität Düsseldorf, Universitätsstr. 1, 40225 Düsseldorf, Germany

E-mail: Christel.Marian@hhu.de

S1 Further Computational Details

For the calculation of the nonradiative rate constants, a time interval of 3 ps with 165536 grid points was chosen and the correlation function was damped with a Gaussian function of 10 cm^{-1} width at half maximum. The temperature was set on 77K and 298K.

S2 (DPEPhos)Cu(PyrTet)

For the (DPEPhos)Cu(PyrTet) complex, the semiempirical Grimme D3 dispersion correction was included in the calculations.[1,2] DFT/MRCI test calculations at the ground-state minimum geometry were made with the R2016 Hamiltonian and standard parameters[3] and the R2018 Hamiltonian with tight parameters.[4] They showed only minor differences (see Figure S1). For the test calculations, 24 roots were calculated with the R2016and 30 singlet and triplet roots with the R2018 Hamiltonian. For the single point calculations at the excited-state minima, only the R2018 Hamiltonian with tight parameters was used and 24 singlet and triplet roots were calculated at each geometry. For all calculations with standard parameters the selection threshold was set to 0.8 E_h in the first run, which only serves for setting up the reference space, and to 1.0 E_h for the final run. With the R2018 Hamiltonians two runs with a selection threshold of 0.8 E_h have been performed.

For the calculations in DCM, the ground state geometry was optimized with the polarizable continuum model (PCM)[5] which is implemented in Gaussian 16.[6] The resulting point charges were adapted for DFT/MRCI calculations and 24 singlet and triplet roots with the R2018 and tight parameters were computed.

The flattening distortion of the (DPEPhos)Cu(PyrTet) complex in the S_1 state is visualized in Figure S2.

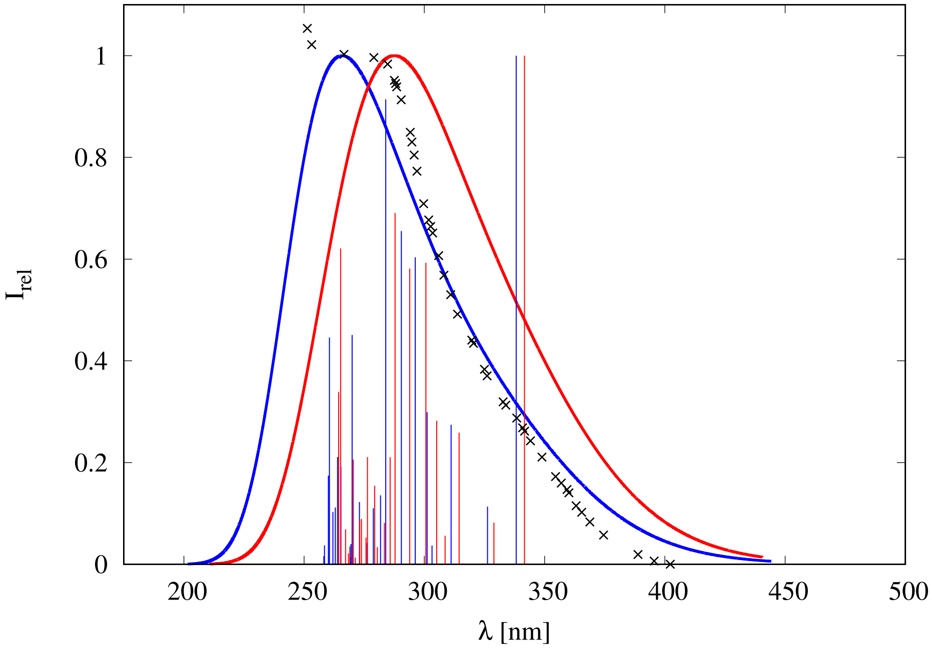

Figure S1: Calculated absorption spectra in vacuum of (DPEPhos)Cu(PyrTet) with the R2016 (red) and R2018 (blue) Hamiltonian in comparison to the experimental spectrum in CH_2Cl_2 (black).

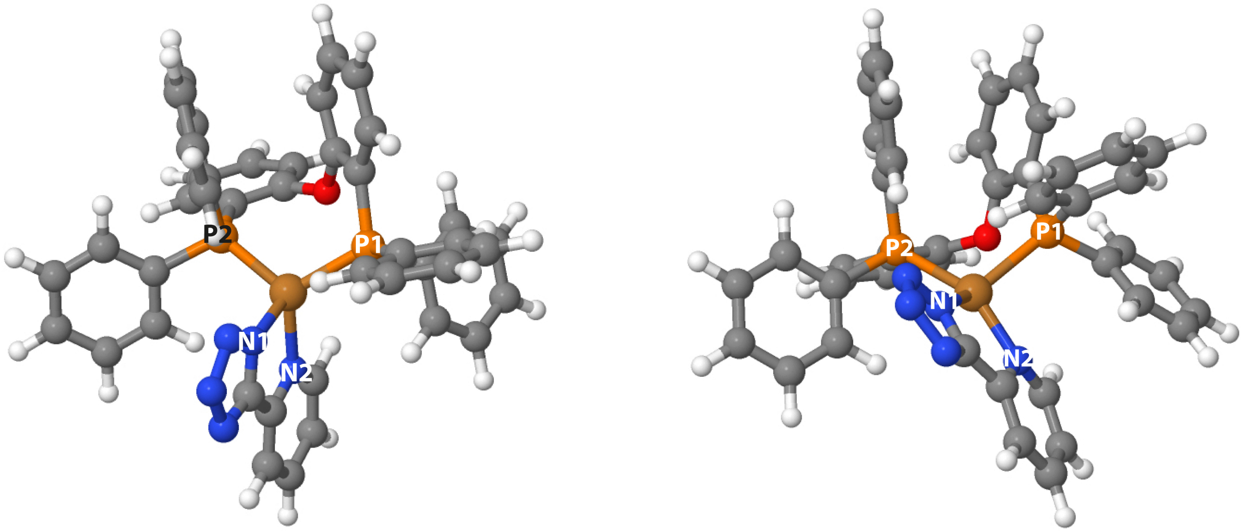

Figure S2: S_0 (left) and S_1 state geometries (right) of the (DPEPhos)Cu(PyrTet) complex in vacuum.

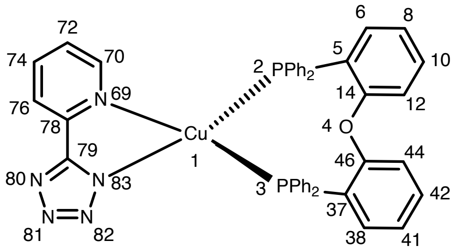

Figure S3: Structure with atom numbers of the (DPEPhos)Cu(PyrTet) complex.

Table S1: Calculated bond lengths (in Å) of the optimized (DPEPhos)Cu(PyrTet) complex in vacuum in comparison to the crystal structure.

bond	S_0	S_1	T_1	crystal structure
C5-C6	1.40	1.40	1.40	1.39
C5-C14	1.40	1.40	1.40	1.38
C6-C8	1.39	1.39	1.39	1.38
C8-C10	1.39	1.39	1.39	1.37
C10-C12	1.39	1.39	1.39	1.38
C12-C14	1.39	1.39	1.39	1.38
C37-C38	1.40	1.40	1.40	1.38
C37-C46	1.41	1.40	1.40	1.39
C38-C40	1.39	1.39	1.39	1.38
C40-C42	1.39	1.39	1.39	1.38
C42-C44	1.39	1.39	1.39	1.37
C44-C46	1.39	1.39	1.39	1.38
C58-C59	1.40	1.40	1.40	1.38
C70-C72	1.39	1.37	1.37	1.37
C72-C74	1.40	1.43	1.43	1.37
C74-C76	1.39	1.40	1.39	1.37
C76-C78	1.40	1.39	1.39	1.38
C78-C79	1.45	1.45	1.44	1.45
Cu1-N69	2.11	1.98	1.95	2.08
Cu1-N83	2.01	1.94	1.94	2.04
Cu1-P2	2.23	2.41	2.38	2.23

Continued on next page

Table S1: Calculated bond lengths (in Å) of the optimized (DPEPhos)Cu(PyrTet) complex in vacuum in comparison to the crystal structure.

bond	S_0	S_1	T_1	crystal structure
Cu1-P3	2.25	2.38	2.36	2.25
C5-P2	1.83	1.83	1.83	1.81
C37-P3	1.84	1.84	1.84	1.83
C14-O4	1.37	1.37	1.37	1.38
C46-O4	1.37	1.37	1.37	1.38
C70-N69	1.33	1.36	1.37	1.33
C78-N69	1.35	1.40	1.41	1.34
C79-N80	1.33	1.33	1.33	1.32
C79-N83	1.34	1.35	1.35	1.33
N80-N81	1.32	1.34	1.34	1.34
N81-N82	1.31	1.29	1.29	1.31
N82-N83	1.32	1.33	1.34	1.34

Table S2: Calculated bond angles (in °) of the optimized (DPEPhos)Cu(PyrTet) complex in vacuum in comparison to the crystal structure.

angle	S_0	S_1	T_1	crystal structure
C5-C6-C8	120.8	120.7	120.7	120.4
C6-C14-C12	121.4	121.3	121.3	121.7
C6-C5-C14	118.3	118.5	118.5	118.3
C6-C8-C10	119.9	119.8	119.8	120.1
C8-C10-C12	120.3	120.5	120.5	120.3
C10-C12-C14	119.3	119.2	119.2	119.2
C37-C38-C40	121.2	121.1	121.1	121.5
C37-C46-C44	121.4	121.5	121.5	121.9
C38-C37-C46	117.7	117.8	117.8	117.3
C38-C40-C42	120.0	120.0	120.0	119.7
C41-C42-C44	119.8	119.9	119.9	120.3

Continued on next page

Table S2: Calculated bond angles (in °) of the optimized (DPEPhos)Cu(PyrTet) complex in vacuum in comparison to the crystal structure.

angle	S_0	S_1	T_1	crystal structure
C42-C44-C46	119.8	119.7	119.7	119.4
C70-C72-C74	118.3	119.7	120.0	119.4
C72-C74-C76	119.3	117.3	117.3	118.9
C74-C76-C78	118.7	120.6	120.7	118.6
C76-C78-C79	123.2	125.6	125.9	123.3
C72-C70-N69	122.7	123.4	123.4	122.9
C76-C78-N69	121.7	121.7	121.7	122.7
C78-C79-N80	129.6	133.5	133.6	128.1
C78-C79-N83	119.9	117.3	117.2	119.7
C79-C78-N69	115.0	112.6	112.4	114.0
C79-N80-N81	104.8	105.2	105.2	104.1
C79-N83-N82	105.7	106.9	106.8	105.1
N80-N81-N82	110.3	111.1	111.2	110.0
N81-N82-N83	108.7	107.7	107.6	108.5
Cu1-N83-N82	141.9	138.8	139.8	141.8
Cu1-N69-C70	129.5	127.6	129.8	129.2
Cu1-N69-C78	111.3	111.9	113.2	113.3
Cu1-N83-C79	112.4	113.1	113.2	112.0
Cu1-P2-C5	111.9	115.1	114.1	107.1
Cu1-P3-C37	119.9	116.2	115.6	120.7
C6-C5-P2	123.7	124.2	124.1	123.7
C14-C5-P2	117.6	117.1	117.2	117.2
C38-C37-P2	122.5	121.4	121.3	122.8
C46-C37-P3	119.6	120.6	120.8	119.9
C5-C14-O4	116.2	115.8	115.8	115.3
C12-C14-O4	122.4	122.9	122.8	123.1
C37-C46-O4	120.1	119.7	119.8	120.1
C44-C46-O4	118.4	118.7	118.7	117.9

Continued on next page

Table S2: Calculated bond angles (in °) of the optimized (DPEPhos)Cu(PyrTet) complex in vacuum in comparison to the crystal structure.

angle	S_0	S_1	T_1	crystal structure
C14-O4-C46	119.8	120.0	119.8	118.4
N69-Cu1-P2	117.4	102.0	105.1	113.2
N69-Cu1-P3	113.9	143.9	139.8	118.1
N83-Cu1-P2	120.2	129.8	129.0	117.4
N83-Cu1-P3	107.3	95.4	94.8	109.0
N69-Cu1-N83	81.3	83.9	83.9	80.5
P2-Cu1-P3	113.0	105.8	106.6	114.4

S3 Trigonal vs. linear NHC-Cu(I)-pyridine complexes

For the $[\text{IPr-Cu-Py}]^+$ and $[\text{IPr-Cu-Pyz}]^+$ complexes the original Grimme Hamiltonian with standard parameters was used in the DFT/MRCI runs.[7] At the ground-state geometry, 21 singlet and 20 triplet roots were calculated and at the excited state geometries 11 singlet and 10 triplet roots were computed.

S4 Carbene-Cu(I)-pyridine complexes

For the -Cu-Py and DAC-Cu-Py complexes, the R2016 Hamiltonian with tight parameters was used.[3] The selection threshold was set on 0.6 E_h in the first and on 0.8 E_h in the second run. In all calculations, 30 singlet and 30 triplet roots were computed.

S5 Carbene-Cu(I)-carbazolide complexes

For all DFT/MRCI calculations of the complexes with the carbazolide ligand and for the CAAC-Cu-Py and DAC-Cu-Py complexes, the R2016 Hamiltonian with tight parameters

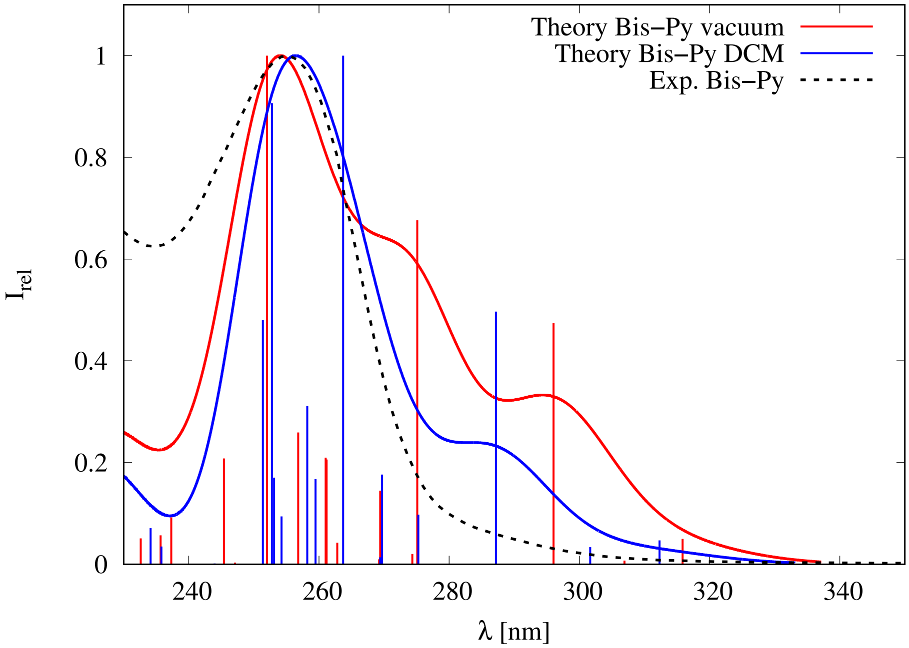

Figure S4: Calculated absorption spectra in vacuum (red) and in DCM (blue) of the [IPr-Cu-Py$_2$]$^+$ complex in comparison to the experimental spectrum in DCM (black).

was used.[3] The selection threshold was set on 0.6 E$_h$ in the first and on 0.8 E$_h$ in the second run. For the CAArC-Cu-Cz and DAC-Cu-Cz complexes 20 singlet and 20 triplet roots and for the other complexes 30 singlet and 30 triplet roots were computed.

S6 Carbene-Cu(I)-chlorides

The DAC-Cu-Cl and NHC-Cu-Cl complexes were optimized with implicit THF solvation of PCM[5] and Gaussian 16.[6] The CAAC$^{\mathrm{Me}}$-Cu-Cl complex is strongly affected by solvation. Solvation effects have to be taken into account in the excited states as well. PCM was used for the ground state, while for the implicit solvation with THF of the S$_1$ and T$_1$ states, the corrected Linear Response (cLR) model was chosen.[8] The PCM and cLR point charges were generated and ulitized for DFT/MRCI calculation with the R2016 Hamiltonian and tight parameters.[3] In all DFT/MRCI calculations 30 singlet and 30 triplet roots were calculated and a selection threshold of 0.8 E$_h$ was chosen.

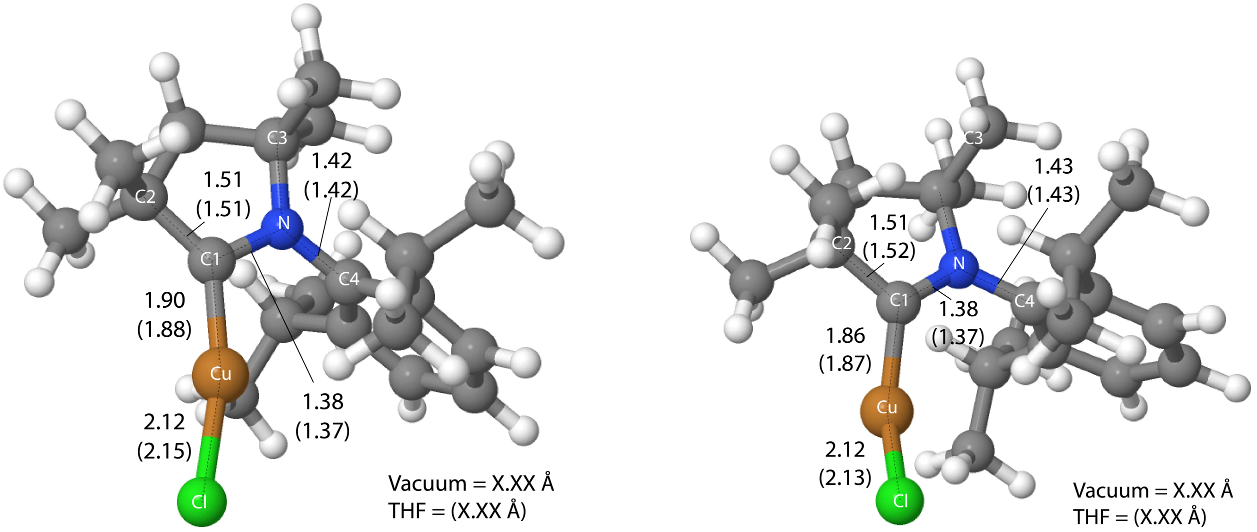

Figure S5: Singlet and triplet excited-state geometries of CAAC$^{\mathrm{Me}}$-Cu-Cl in vacuum showing selected bond lengths (in Å units): Left S_1, right T_1. Corresponding values for THF solution in the cLR environment are shown in parentheses.

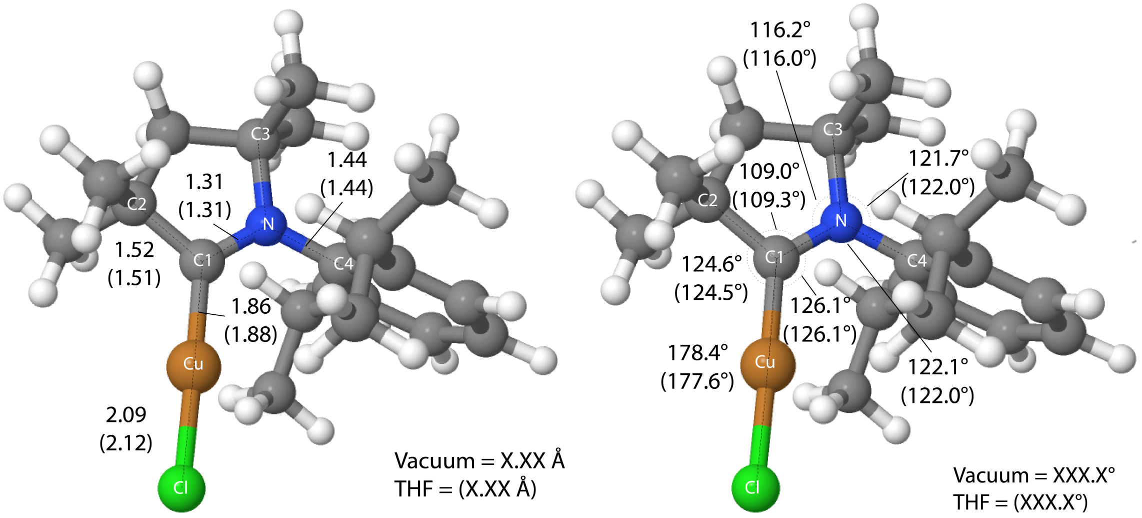

Figure S6: Ground-state geometry of CAAC$^{\mathrm{Me}}$-Cu-Cl in vacuum showing selected bond lengths (left in Å units) and bond angles (right). Corresponding values for THF solution in the PCM are displayed in parentheses.

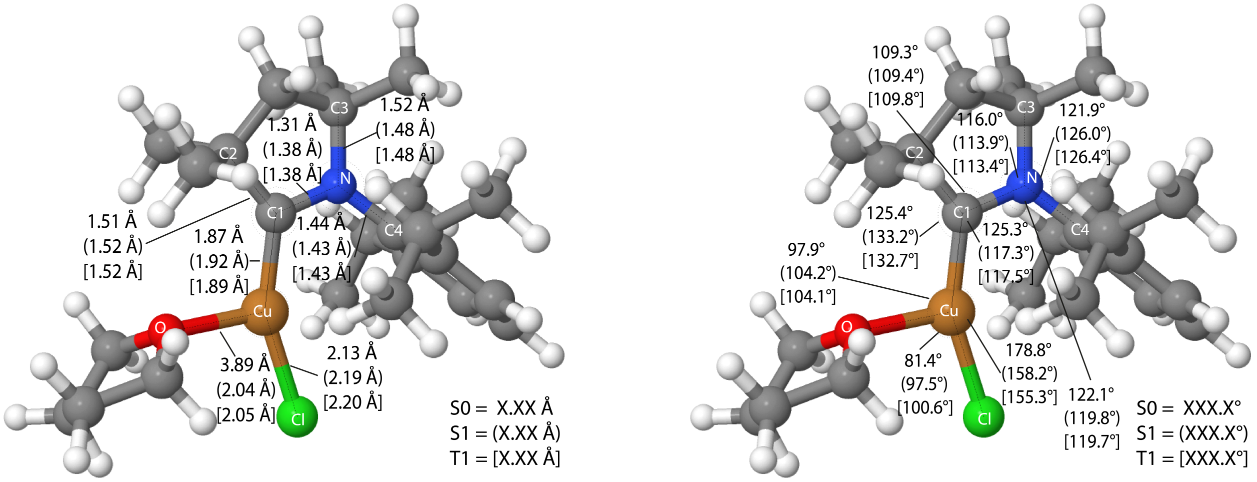

Figure S7: CAAC^{Me}-Cu-Cl with an explicit THF molecule showing selected bond lengths (left in Å units) and bond angles (right) of the ground state and the first excited singlet and triplet states in implicit THF solution.

References

(1) Grimme, S.; Antony, J.; Ehrlich, S.; Krieg, H. A consistent and accurate ab initio parametrization of density functional dispersion correction (DFT-D) for the 94 elements H-Pu. *J. Chem. Phys.* **2010**, *132*, 154104.

(2) Grimme, S. Density functional theory with London dispersion corrections. *WIREs Comput. Mol. Sci.* **2011**, *1*, 211–228.

(3) Lyskov, I.; Kleinschmidt, M.; Marian, C. M. Redesign of the DFT/MRCI Hamiltonian. *J. Chem. Phys.* **2016**, *144*, 034104.

(4) Heil, A.; Kleinschmidt, M.; Marian, C. M. On the performance of DFT/MRCI Hamiltonians for electronic excitations in transition metal complexes: The role of the damping function. *J. Chem. Phys.* **2018**, *149*, 164106.

(5) Miertuš, S.; Scrocco, E.; Tomasi, J. Electrostatic interaction of a solute with a continuum. A direct utilizaion of AB initio molecular potentials for the prevision of solvent effects. *Chem. Phys.* **1981**, *55*, 117 – 129.

(6) Frisch, M. J. et al. Gaussian 16 Revision B.01. 2016; Gaussian Inc. Wallingford CT.

(7) Grimme, S.; Waletzke, M. A Combination of Kohnham Density Functional Theory and Multi-Reference Configuration Interaction Methods. *J. Chem. Phys.* **1999**, *111*, 5645–5655.

(8) Caricato, M.; Mennucci, B.; Tomasi, J.; Ingrosso, F.; Cammi, R.; Corni, S.; Scalmani, G. Formation and relaxation of excited states in solution: A new time dependent polarizable continuum model based on time dependent density functional theory. *J. Chem. Phys.* **2006**, *124*, 124520.